Floquet dynamical phase transition and entanglement spectrum

R. Jafari [1,2,3,*] and Alireza Akbari [4,5,1,†]

[1]*Department of Physics, Institute for Advanced Studies in Basic Sciences (IASBS), Zanjan 45137-66731, Iran*
[2]*Department of Physics, University of Gothenburg, SE 412 96 Gothenburg, Sweden*
[3]*Beijing Computational Science Research Center, Beijing 100094, China*
[4]*Max Planck Institute for the Chemical Physics of Solids, D-01187 Dresden, Germany*
[5]*Max Planck POSTECH Center for Complex Phase Materials, and Department of Physics, POSTECH,*
Pohang, Gyeongbuk 790-784, Korea

We explore both pure and mixed state Floquet dynamical quantum phase transitions (FDQFTs) in the one-dimensional p-wave superconductor with a time-driven pairing phase. In the Fourier space the model is recast to the noninteracting quasispins subjected to a time-dependent effective magnetic field. We show that FDQFTs occur within a range of driving frequency without resorting to any quenches. Moreover, FDQFTs appear in the region where quasispins are in the resonance regime. In the resonance regime, the population completely cycles the population between the spin down and up states. Additionally, we study the conditions for the appearance of FDQFTs using the entanglement spectrum and purity entanglement measure. Our results imply that the entanglement spectrum can truly capture the resonance regime where FDQFTs occur. Particularly, the dynamical topological region results in the degeneracy of the entanglement spectrum. It is shown that the boundary of the driven frequency range, over which the system reveals FDQFTs, is signaled by the purity entanglement measure.

I. INTRODUCTION

Quantum phase transition (QPT), in a similar fashion as a classical phase transition, is one of the most intriguing research topics in condensed-matter physics [1]. It is characterized by signaling nonanalytic behaviors in some physical properties of the system [2] and is often accompanied by a divergence in some correlation functions. But, the quantum systems possess additional "quantum correlations" which do not exist in classical counterparts [3]. Consequently, quantum correlations could be useful to investigate the quantum phase transition [4–9].

Entanglement is a type of quantum correlation first signified by Schrödinger in 1935 [10] as a particular feature of quantum mechanics. As a direct measure of quantum correlations, it displays nonanalytic behavior such as discontinuity at the quantum critical points [11–13]. In the past decade, the subject of several pieces of research was to explore the behavior of entanglement near and at the quantum critical point for different spin models [11,14–16] as well as itinerant systems [17–19]. Furthermore, purity entanglement measure [20–22] and entanglement spectrum (ES) [23–27] are introduced for quantifying the characteristics of quantum entanglement in many-body systems.

Recently, the concept of dynamical quantum phase transitions (DPQTs) have been introduced as nonequilibrium

counterparts of thermal phase transitions [28,29]. The notion of DQPT emanates from the similarity between the equilibrium partition function of a system and Loschmidt amplitude, which measures the overlap between an initial state and its time-evolved one [28–42]. While the equilibrium phase transition is characterized by nonanalyticities in the thermal free energy, the DQPT is signaled by the nonanalytical behavior of dynamical free energy, in which real time plays the role of the control parameter [43–46]. Furthermore, analogous to order parameters at equilibrium quantum phase transition, a dynamical topological order parameter is proposed to capture DQPTs [47,48]. The DTOP is quantized and its unit magnitude jumps at the time of DQPT reveal the topological characteristic feature of DQPT [47–50]. This dynamical topological order parameter is extracted from the "gauge-invariant" Pancharatnam geometric phase associated with the Loschmidt amplitude [47,48,51].

More recently, significant theoretical [52–70] and experimental [71–77] endeavors have focused on DQPTs. On the theoretical front, most research is devoted to study the DQPTs of both slow and sudden quantum quenches of the Hamiltonian. Furthermore, few works attempt to provide a link between sudden quench DQPTs and entanglement [78,79], entanglement entropy [72,80,81], and entanglement spectrum [81–84]. Lately, time-periodic driving and the corresponding Floquet theory has attracted great attention [85–88]. The study of time-periodically driven closed quantum systems in the context of the Floquet theory is one of the most attractive areas of developing nonequilibrium research.

_____
*jafari@iasbs.ac.ir; rohollah.jafari@gmail.com
†akbari@postech.ac.kr

Despite considerable investigation of many aspects of DQPTs [52,54–66,70], comparatively, little attention has been directed toward dynamical quantum phase transition in Floquet systems which are called Floquet DQPTs [85–88]. To make progress, more studies are needed, specifically, the exactly solvable models play an important role.

The main aim of this study is to find the connection between Floquet DQPTs and purity entanglement measure and entanglement spectrum. Such contributions can bring several new realizations to the subject. Here we study analytically both pure and mixed state Floquet dynamical quantum phase transitions (FDQFTs) in the one-dimensional p-wave superconductor with a time-driven pairing phase. We show that FDQFTs occur without requiring any quenches at the region where the population between spin down and up states is completely cycled. We also investigate the conditions for the appearance of DQPTs using entanglement spectrum and purity entanglement measures. The range of driving frequency over that system is dynamically topological and the dynamical topological QPT (DTQPT) arises, as well as, the region where DTQPT happens, signaled by the degeneracy of the entanglement spectrum, can truly be detected by the entanglement spectrum and the purity entanglement measures.

II. THEORETICAL MODEL

The Hamiltonian of a one-dimensional p-wave superconductor with time-dependent pairing phase (magnetic flux) is given as [89]

$$
\mathcal{H} = \sum_{j=1}^{N}\left[\left(\frac{\mathcal{W}}{2}c_j^\dagger c_{j+1} - \frac{\Delta}{2}e^{-i\theta(t)}c_j^\dagger c_{j+1}^\dagger + \text{H.c.}\right) - \mu\left(c_j^\dagger c_j - \frac{1}{2}\right)\right],
\tag{1}
$$

where c_j ($c_j^\dagger$) is the fermion creation (annihilation) operator, N is the number of lattice sites, and μ is the chemical potential. The hopping and pairing amplitudes are w and Δ, respectively. The phase factor $\theta(t)$ in the pairing terms is the vector potential, interpreting as an Aharonov-Bohm flux $\Phi(t) = N\theta(t)$ piercing the ring [90]. This model can be mapped to the periodically time-dependent extended XY spin model via a Jordan-Wigner transformation. To diagonalize the fermionic Hamiltonian in Eq. (1) we perform a Fourier transform $c_j = \frac{1}{\sqrt{N}}\sum_k c_k e^{ikj}$ and $c_j^\dagger = \frac{1}{\sqrt{N}}\sum_k c_j^\dagger e^{-ikj}$. Considering antiperiodic boundary conditions ($c_{j+N} = -c_j$), results in the wave number $k = (2p-1)\pi/N$, where p runs from 1 to $N/2$. Introducing fermionic two-component $\Gamma_k^\dagger = (c_k^\dagger, c_{-k})$, the Hamiltonian of Eq. (1) can be written as the sum of N noninteracting terms

$$
\mathcal{H} = \sum_k \Gamma_k^\dagger H_k(t)\Gamma_k,
\tag{2}
$$

where the Bloch Hamiltonian $H_k(t)$ is defined as

$$
H_k(t) = \tfrac{1}{2}\{h_{xy}(k)[\sin(\omega t)\sigma_x - \cos(\omega t)\sigma_y] + h_z(k)\sigma_z\},
$$

with $h_z(k) = \mathcal{W}\cos(k) - \mu$ and $h_{xy}(k) = \Delta\sin(k)$, where $\sigma_{\alpha=0,x,y,z}$ are Pauli matrices. We should mention that Eq. (2) expresses the Hamiltonian of interacting fermions system [Eq. (1)] mapped to the sum of noninteracting quasispins imposed by the time-dependent effective magnetic field. The single particle quasispin Hamiltonian $H_k(t)$ is exactly the Schwinger-Rabi model of a spin in a rotating magnetic field [91]. The exact solution to the time-dependent Schrödinger equation $i\frac{d}{dt}|\psi(k,t)\rangle = H_k(t)|\psi(k,t)\rangle$ is achieved by going to the rotating frame given by the periodic unitary transformation [92]

$$
U_R(t) = e^{i\omega(\sigma_0 - \sigma_z)t/2} = \begin{pmatrix} 1 & 0 \\ 0 & e^{i\omega t} \end{pmatrix}
\tag{3}
$$

to obtain the time-independent Floquet Hamiltonian H_F as

$$
H_k^F = U_R^\dagger(t)H_k(t)U_R(t) - iU_R^\dagger(t)\frac{dU_R(t)}{dt}
$$
$$
= -\frac{1}{2}\{h_{xy}(k)\sigma_y - [h_z(k) - \omega]\sigma_z - \omega\sigma_0\}.
\tag{4}
$$

The eigenvalues and eigenvectors of the Floquet Hamiltonian H_k^F are given by

$$
\varepsilon_k^\pm = \frac{1}{2}\big[\omega \pm \sqrt{h_{xy}^2(k) + [h_z(k) - \omega]^2}\big]
\tag{5}
$$

and

$$
|\chi_k^\pm\rangle = \frac{1}{N_k}[h_{xy}(k)|\mp\rangle + i\eta_z(k)|\pm\rangle],
\tag{6}
$$

respectively. Here we define

$$
N_k = \sqrt{\eta_z^2(k) + h_{xy}^2(k)}, \quad \eta_z(k) = [h_z(k) - 2\varepsilon_k^-],
$$

and $|\pm\rangle$ are the eigenstates of σ_z. In the original frame, the Floquet states of the Hamiltonian $H_k(t)$ is given by

$$
|\psi_k^\pm(t)\rangle = U_R(t)e^{-iH_k^F t}|\chi_k^\pm\rangle = e^{-i\varepsilon_k^\pm t}U_R(t)|\chi_k^\pm\rangle.
\tag{7}
$$

Consequently, the initial and time-evolved ground states of the original Hamiltonian are obtained as follows:

$$
|\psi^-(t)\rangle = \Pi_k|\psi_k^-(t)\rangle = \Pi_k e^{-i\varepsilon_k^- t}U_R(t)|\chi_k^-\rangle,
$$
$$
|\psi^-(0)\rangle = \Pi_k|\chi_k^-\rangle.
\tag{8}
$$

Moreover, in fermion language the ground state of the proposed time-dependent Hamiltonian Eq. (1) is given as

$$
|\psi^-(t)\rangle = \prod_{k>0}[u_k(t,\omega) + v_k(t,\omega)c_k^\dagger c_{-k}^\dagger]|0\rangle,
\tag{9}
$$

where $u_k(t,\omega) = h_{xy}(k)e^{-i\varepsilon_k^- t}/N_k$ and $v_k(t,\omega) = i\eta_z(k)e^{-i\varepsilon_k^- t}e^{i\omega t}/N_k$. If we assume the system initially prepared in $|-\rangle$ state at $t = 0$, the probability of the transition from state $|-\rangle$ to state $|+\rangle$ (spin-flip probability) is given as

$$
P_f = \frac{h_{xy}^2}{\Omega_R}\sin^2\left(\frac{\Omega_R t}{2}\right), \quad \Omega_R = \sqrt{h_{xy}^2(k) + [h_z(k) - \omega]^2}.
\tag{10}
$$

Note that whenever $h_z = \omega$, the spin-flip (Rabi transition) probability becomes a maximum possible value $\Omega_R = 1$. In such a resonance situation, the period of oscillation $T_R = 2\pi/\Omega_R$ is different from the driving period [91]. In other words, the population at resonance completely cycles the population between the two spin down and up states, while for $h_z \neq \omega$, the down state $|-\rangle$ is never completely depopulated.

III. DYNAMICAL QUANTUM PHASE TRANSITION

As mentioned, the concept of a DQPT is extracted from the analogy between the partition function of an equilibrium system $Z(\beta) = \mathrm{Tr}[e^{-\beta\mathcal{H}}]$ and the boundary quantum partition function $Z(z) = \langle\psi_0|e^{-z\mathcal{H}}|\psi_0\rangle$ with $|\psi_0\rangle$ a boundary state and $z \in \mathbb{C}$. When $z = it$, the boundary quantum partition function becomes equivalent to a Loschmidt amplitude (LA) $\mathcal{L}(t) = \langle\psi_0|e^{-i\mathcal{H}t}|\psi_0\rangle$, denoting the overlap between the initial state $|\psi_0\rangle$ and the time-evolved one $|\psi_0(t)\rangle$ [28]. Heyl *et al.* [28] showed that, similar to the thermal free energy, a dynamical free energy can be defined as

$$g(t) = -\frac{1}{2\pi}\int_{-\pi}^{\pi} dk \ln|\mathcal{L}_k(t)|^2,$$

where real time t plays the role of the control parameter. DQPTs are simply signaled by nonanalytical behavior of $g(t)$ as a function of time, evincing in characteristic cusps in $g(t)$ or one of its time derivatives. These cusps are followed by zeros of $\mathcal{L}(t)$, known in statistical physics as Fisher zeros of the partition function [93]. In this section we search both pure and mixed state Floquet DQPTs in a proposed time-dependent Hamiltonian Eq. (1) to study features of DQPTs in the quantum Floquet systems.

A. Pure state dynamical topological quantum phase transition

A straightforward calculation yields the exact expression of the Loschmidt amplitude corresponding to the ground state of the proposed model as follows:

$$\mathcal{L}(t) = \langle\psi^-(0)|\psi^-(t)\rangle = \Pi_k \mathcal{L}_k(t), \quad (11)$$

with

$$\mathcal{L}_k(t) = \langle\chi_k^-|\psi_k^-(t)\rangle = e^{-i\varepsilon_k^- t}\langle\chi_k^-|U_R(t)|\chi_k^-\rangle$$
$$= \left[\frac{h_{xy}^2(k) + \eta_z^2(k)e^{i\omega t}}{h_{xy}^2(k) + \eta_z^2(k)}\right]e^{-i\varepsilon_k^- t}.$$

Analyzing Eq. (11) reveals that the zeros of $\mathcal{L}(t)$ at which DQPTs occur take place at critical times:

$$t_n^* = (2n+1)\frac{\pi}{\omega} = \left(n + \frac{1}{2}\right)t^*, \quad t^* = 2\pi/\omega, \quad n\in\mathbb{Z},$$
$$(12)$$

only whenever there is a mode k^* that satisfies $h_z(k^*) = \omega$. Also, a critical mode k_c exists when $\cos(k^*) = (\omega + \mu)/\mathcal{W}$, and results $\omega_1 \leqslant \omega \leqslant \omega_2$, with $\omega_1 = -\mathcal{W} - \mu$ and $\omega_2 = \mathcal{W} - \mu$. The condition $h_z(k) = \omega$ is equivalent to the resonance characteristic in the Schwinger-Rabi model of a quasispin in a rotating effective magnetic field [91]. Thus, two regimes emerge in the proposed time-dependent Hamiltonian Eq. (1). First, the resonance regime where the probability of the quasispins flip becomes the maximum possible value. Second, the nonresonance regime where the quasispin population does not completely cycle the population between the spin down and up states. We should stress that DQPTs region coincides with the adiabatic regime where the quasispins trace the time-dependent effective magnetic field. While in the region where quasispins in a rotating magnetic field feel a constant effective Zeeman field no DQPTs occur [88].

The density plot of Loschmidt echo (squared modulus of LA) $R_k(t)$, and dynamical free energy $g(t)$, are shown in Figs. 1(a)–1(c). It is clear that, in the resonance regime [Figs. 1(a) and 1(b)] there exist critical points k^* and t^*, where $\mathcal{L}_{k^*}(t^*)$ becomes zero. In contrast, there is no such critical point in a nonresonance regime. As shown in Fig. 1(c), the nonanalyticities in the dynamical free energy and DQPT arise for the driving frequency at which the quasispins are in the resonance situation.

As stated in the Introduction, a dynamical topological order parameter (DTOP) has been proposed to indicate that the topological features emerge in DQPTs. The DTOP represents integer values as a function of time and shows unit magnitude jumps at the critical times at which the DQPTs appear. The DTOP is a momentum-space winding number of the Pancharatnam geometric phase which serves as a dynamical analog of a topological order parameter in two-banded Bogoliubov–de Gennes models that experiences a DQPT after a a sudden change in the band structure parameters. The integer values of DTOP changes only at DQPTs which reveals how the topology of the underlying Hamiltonian has changed during the quench (evolution) [47,48,51].
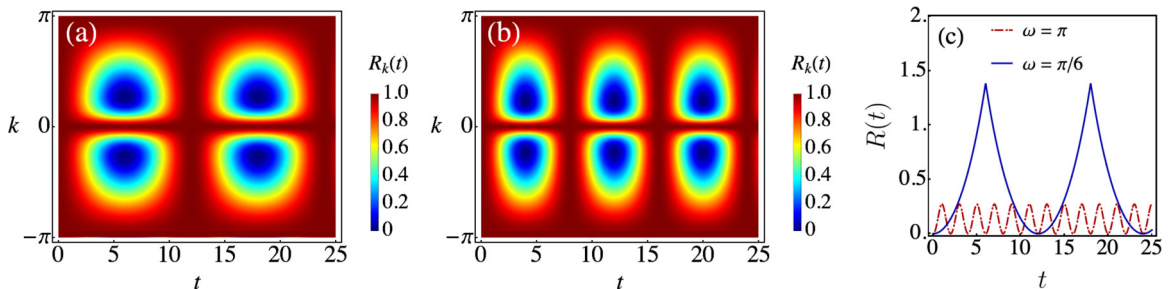

FIG. 1. The density plot of Loschmidt echo versus t and k for (a) $\omega = \pi/6$ and (b) $\pi/4$. (c) The dynamical free energy $g(t)$ versus t for $\omega = \pi/6$ (solid line) and $\omega = \pi$ (dotted line).
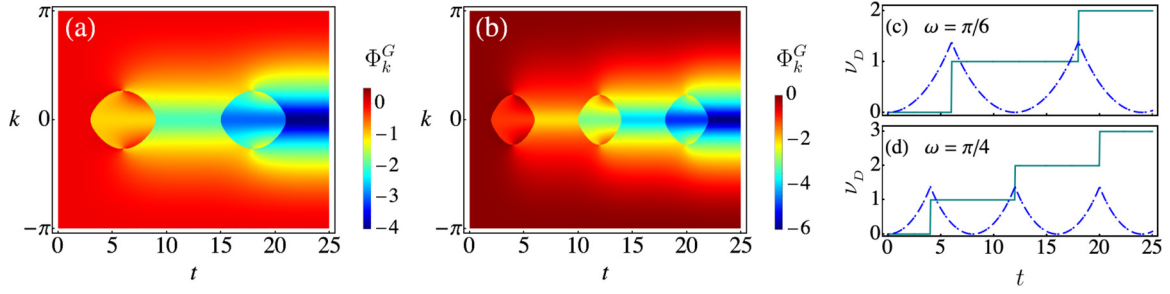
FIG. 2. The density plot of geometric phase versus k and t for (a) $\omega = \pi/6$ and (b) $\pi/4$. The dynamical topological order parameter versus time for (c) $\omega = \pi/6$ and (d) $\omega = \pi/4$ [dashed lines show the dynamical free energy $g(t)$ versus t].

The dynamical topological order parameter is given [47]

$$\nu_D(t) = \frac{1}{2\pi} \int_0^\pi \frac{\partial \phi^G(k,t)}{\partial k} dk, \tag{13}$$

where the geometric phase $\phi^G(k,t)$ is gained from the total phase $\phi(k,t)$ by subtracting the dynamical phase $\phi^D(k,t)$: $\phi^G(k,t) = \phi(k,t) - \phi^D(k,t)$. The total phase $\phi(k,t)$ is the phase factor of LA in its polar coordinates representation, i.e.,

$$\mathcal{L}_k(t) = |\mathcal{L}_k(t)| e^{i\phi(k,t)}$$

and

$$\phi^D(k,t) = -\int_0^t \langle \psi_k^-(t')|H_k^F|\psi_k^-(t')\rangle dt',$$

in which $\phi(k,t)$ and $\phi^D(k,t)$ can be calculated as follows:

$$\phi(k,t) = -\varepsilon_k^- t + \tan^{-1}\left(\frac{\eta_z^2(k)\sin(\omega t)}{h_{xy}^2(k) + \eta_z^2(k)\cos(\omega t)}\right),$$

$$\phi^D(k,t) = \left[\frac{h_{xy}^2(k) + h_z(k)[h_z(k) - \omega]}{2\Omega_R}\right] t. \tag{14}$$

The geometric phase $\phi^G(k,t)$ and $\nu_D(t)$ have been illustrated in Figs. 2(a)–2(c) for different values of the driving frequencies in the resonance regime, showing excellent agreement with the analytical result. The plots display singular changes in successive critical times t_n^* at critical momentum k^*, which characterizes the topological aspects of DQPTs.

B. Mixed state dynamical topological phase transition

In experiments [71,72], the initial state of far-from-equilibrium, in which the system is prepared, is usually not a pure state but rather a mixed state. Consequently, on the theoretical front, a generalized Loschmidt amplitude (GLA) for mixed thermal states has been established, which perfectly yields the nonanalyticities appearing in the pure state DQPTs [51,94,95]. Now we study the mixed state Floquet DQPTs in the time-dependent Hamiltonian, Eq. (1). The GLA for thermal mixed state is described by

$$\mathcal{G}L(t) = \prod_k \mathcal{G}L_k(t) = \prod_k \text{Tr}[\rho_k(0)U(t)], \tag{15}$$

where $\rho_k(0)$ is the mixed state density matrix at time $t = 0$, and $U(t)$ is the time-evolution operator. The time-evolution operator and the mixed state density matrix of Hamiltonian in

Eq. (1) are given by

$$U(t) = U_R(t)e^{-iH_k^F t} = e^{i\omega(\sigma_0 - \sigma^z)t/2}e^{-iH_k^F t} \tag{16}$$

and

$$\rho_k(0) = \frac{e^{-\beta H_k^F}}{\text{Tr}(e^{-\beta H_k^F})} = \frac{1}{2}\left[\sigma_0 - \tanh\left(\frac{\beta \Delta_k}{2}\right)\hat{n}_k \cdot \vec{\sigma}\right], \tag{17}$$

respectively. Here $H_k^k = \frac{1}{2}(\omega\sigma_0 + \Delta_k\hat{n}_k \cdot \vec{\sigma})$ with $\Delta_k = |\varepsilon_k^+ - \varepsilon_k^-|$, $\hat{n}_k = [0, -h_{xy}(k), h_z(k) - \omega]/\Delta_k$ and $\beta = 1/T$ is the inverse temperature with Boltzmann constant $K_B = 1$. A rather lengthy calculation results in an exact expression for GLA, which is represented by

$$\mathcal{G}L_k(t) = \frac{1}{\Delta_k}\tanh\left(\frac{\beta\Delta_k}{2}\right)[\Upsilon_1(k,t) + i\Upsilon_2(k,t)], \tag{18}$$

where $\Upsilon_1(k,t)$ and $\Upsilon_2(k,t)$ are identified as

$$\Upsilon_1(k,t) = \Delta_k \cos\left(\frac{\omega t}{2}\right)\cos\left(\frac{\Delta_k t}{2}\right)$$
$$- [h_z(k) - \omega]\sin\left(\frac{\omega t}{2}\right)\sin\left(\frac{\Delta_k t}{2}\right),$$

$$\Upsilon_2(k,t) = \Delta_k \cos\left(\frac{\omega t}{2}\right)\sin\left(\frac{\Delta_k t}{2}\right)$$
$$+ [h_z(k) - \omega]\sin\left(\frac{\omega t}{2}\right)\cos\left(\frac{\Delta_k t}{2}\right).$$

The density plot of modulus of GLA has been displayed versus time t and k in Figs. 3(a)–3(f) for different values of β and driving frequencies in resonance regime $\omega = \pi/6$ and $\omega = \pi/4$. As seen, the critical points k^* and t^*, where GLA becomes zero, are exactly the same as the corresponding one in LA. Therefore, we expect that the mixed state DQPTs appear in the resonance regime even at finite temperatures. The comparison of Figs. 1(a) and 1(b) with Figs. 3(a)–3(f) reveals that GLA is deformed versus time. Our numerical results show that the deformation is enhanced by increasing the temperature and time. The dynamical free energy of GLA has been depicted versus time in Fig. 4(a) for different values of β and driving frequency $\omega = \pi/4$. It can be clearly seen that GLA correctly captures the critical mode k^* and critical time t^* observed during the pure state DQPT, but the height of cusps increases by increasing temperature. It should be stressed that as the temperature gets smaller than the effective temperature associated with the minimum energy gap, the
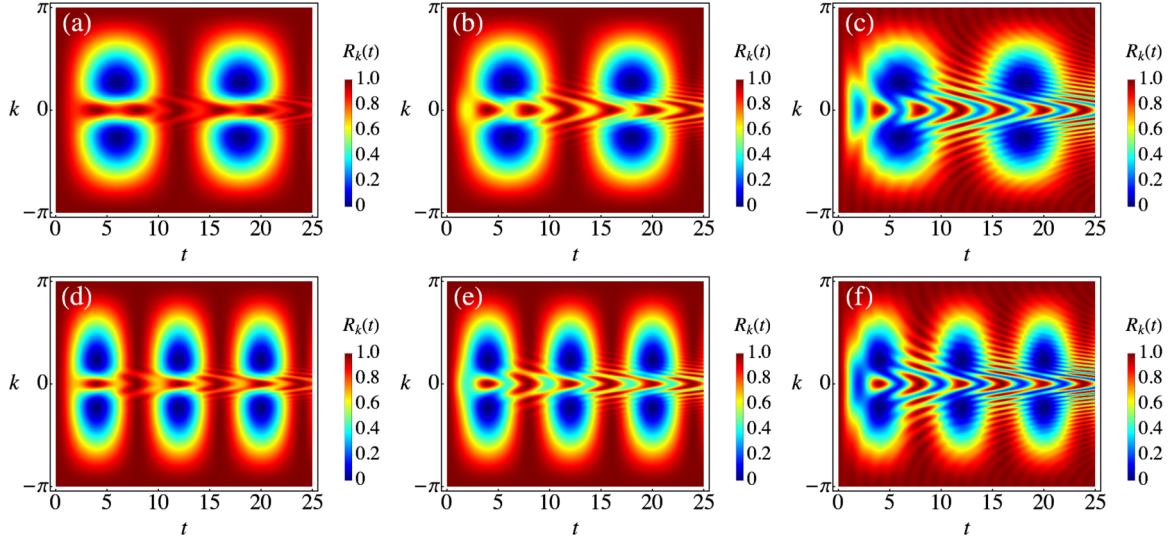
FIG. 3. The Loschmidt echo of mixed state versus k and t for (a) $\omega = \pi/6$ and $\beta = 1$, (b) $\omega = \pi/6$ and $\beta = 2$, (c) $\omega = \pi/6$ and $\beta = 3$, (d) $\omega = \pi/4$ and $\beta = 1$, (e) $\omega = \pi/4$ and $\beta = 2$, and (e) $\omega = \pi/4$ and $\beta = 3$.

critical modes and times of the mixed state DQPT remain unaffected. For higher temperatures the hallmark of DQPT is wiped out, which express a traverse to a the regime without DQPT.

Moreover, for mixed state DQPT a topological invariant has been proposed to lay out its topological characteristics [51]. In the mixed state DQPT the total phase and dynamical phase are given as

$$\phi(k, \beta, t) = \text{Arg}\{\text{Tr}[\rho(k, \beta, 0)U(t)]\}$$

and

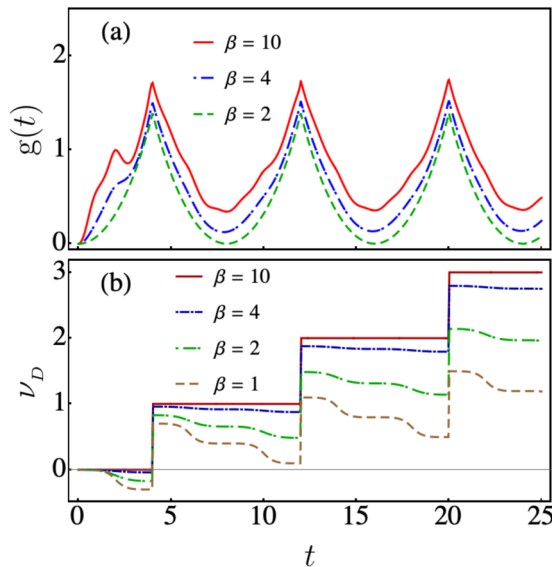$$\phi^D(k, \beta, t) = -\int_0^t \text{Tr}[\rho(k, \beta, t')H(k, t')]dt',$$

FIG. 4. (a) The dynamical free energy of mixed state $g(t)$ versus time for different values of β. (b) The mixed state dynamical topological order parameter versus time for different values of β and $\omega = \pi/4$.

respectively. The topological invariant $\nu_D(t)$ can be calculated using Eq. (12) for the mixed state in which

$$\phi^G(k, \beta, t) = \phi(k, \beta, t) - \phi^D(k, \beta, t).$$

After a lengthy calculation, one can obtain the total phase $\phi(k, \beta, t)$ and the dynamical phase $\phi^D(k, \beta, t)$ as follows:

$$\phi(k, \beta, t) = \text{Arg}\{\text{Tr}[\rho(k, \beta, 0)U(t)]\}$$
$$= \tan^{-1}\left[\left(\frac{\Upsilon_2(k, t)}{\Upsilon_1(k, t)}\right)\tanh\left(\frac{\beta \Delta_k}{2}\right)\right],$$

$$\phi^D(k, \beta, t) = -\int_0^t dt'\text{Tr}[\rho(k, \beta, t')H(k, t')]$$
$$= \tanh\left(\frac{\beta \Delta_k}{2}\right)\left[\frac{h_z(k)[h_z(k) - \omega] + h_{xy}^2(k)}{2\Delta_k}\right]t.$$
$$(19)$$

In Fig. 4(b) the mixed state topological invariant has been plotted for driving frequencies $\omega = \pi/4$ and different values of β. It can be seen clearly that $\nu_D(t)$ exhibits a nearly perfect quantization (unit jump) as a function of time between the two DQPT times. When temperature is smaller than the effective temperature, associated with the minimum energy gap, the quantized structure of $\nu_D(t)$ can be observed. Although sudden jumps of $\nu_D(t)$ is present at higher temperatures, it does not show a quantized value to display a topological character. Consequently, mixed state DQPT exist and are signaled by nearly a quantized mixed state dynamical topological order parameter, when the temperature is below a crossover temperature.

IV. ENTANGLEMENT

As stated, characterization of quantum phase transitions (QPTs) and quantum phases via purity entanglement measures [20–22] and ES [23–27] is one of the most intriguing research topics in condensed-matter physics [96]. In this section we study the purity entanglement measure and entanglement

spectrum as a generalization of entanglement in the time-dependent Hamiltonian Eq. (1). We show that both purity entanglement measure and entanglement spectrum can detect the boundary of the driven frequency range over which DQPTs take place.

A. Entanglement spectrum

In the following we focus on the entanglement spectrum of the proposed time-dependent Hamiltonian Eq. (1). To calculate it, we should obtain two $l \times l$ correlation matrices C and F with the matrix elements $C_{mn} = \langle \psi(t)|c_m^\dagger c_n|\psi(t)\rangle$ and $F_{mn} = \langle \psi(t)|c_m^\dagger c_n^\dagger|\psi(t)\rangle$, respectively. Here $1 \leqslant m, n \leqslant l$, and entanglement spectrum can be obtained from a $2l \times 2l$ correlation matrix defined as

$$\mathcal{C}_l(t) = \begin{pmatrix} I - C & F \\ F^\dagger & C \end{pmatrix}, \tag{20}$$

where I is the $l \times l$ identity matrix. The single-particle entanglement spectrum is obtained by the eigenvalues of the correlation matrix $\mathcal{C}_l(t)$ [97], and they come in pairs of $\xi_m(t)$ and $1 - \xi_m(t)$ [84]. Moreover, the entanglement entropy of the subblock of size l is given by

$$S_l(t) = -\mathrm{Tr}[\mathcal{C}_l(t) \log_2 \mathcal{C}_l(t)] = -\sum_m^{2l} \xi_m(t) \log_2 [\xi_m(t)].$$

Having obtained the time evolved state in Eq. (9), the correlation matrix elements can be calculated as follows:

$$C_{mn} = \frac{1}{L} \sum_k |v_k(t,\omega)|^2 e^{-ik(m-n)},$$

$$F_{mn} = \frac{1}{L} \sum_k v_k^*(t,\omega) u_k(t,\omega) e^{-ik(m-n)}.$$

The knowledge of the correlation matrix $\mathcal{C}_l(t)$ enables us to calculate the entanglement spectrum. We have calculated the eigenvalues of the correlation matrix for $l = 40$. Our numerical calculation shows that the eigenvalues of the correlation matrix are time independent. In addition, the derivative of all the eigenvalues with respect to the driven frequency show divergence at the boundary of the resonance regime where DQPTs happen.

The four middle eigenvalues of the correlation matrix are shown in Fig. 5(a), and the derivative of two middle eigenvalues of correlation matrix have been plotted in Fig. 5(b) for $\mathcal{W} = \pi$ and $\mu = \pi/2$. As seen, the boundary resonance region, i.e., $\omega_1 = -3\pi/2$ and $\omega_2 = \pi/2$, have been signaled by the derivative of the eigenvalues with respect to the driven frequency. As evidence, two middle eigenvalues of the correlation matrix are degenerate at the resonance region. This phenomenon is similar to what happened in the entanglement spectrum crossing [23,81]. In the entanglement spectrum crossing phenomena, the topological phase results in degeneracies of low-lying entanglement spectrum [98]. In other words, the low-lying entanglement spectrum will be $1/2$ in the topological phase. Thus, the entanglement spectrum is able to detect the topological phase, i.e., the resonance region where dynamically is topological. Furthermore, it is noteworthy to mention that the entanglement entropy is zero in the nonresonance regime and is one in the resonance regime. This
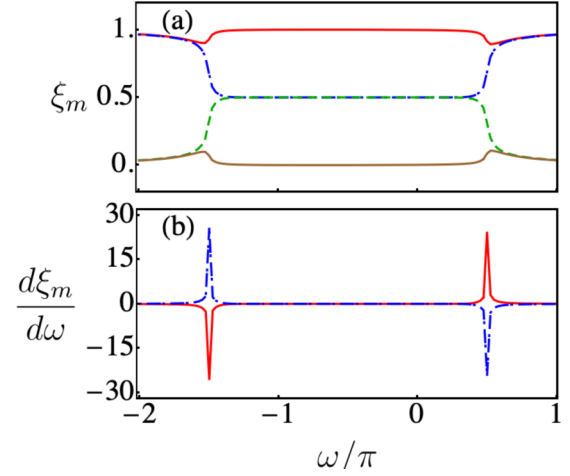

FIG. 5. (a) The four middle eigenvalues of entanglement spectrum versus ω. (b) The derivative of two middle eigenvalues of entanglement spectrum with respect to driven frequency versus ω. We set $\mathcal{W} = \pi$ and $\mu = \pi/2$.

means the system at the resonance regime, where dynamically topological, is entangled while it is disentangled in the nonresonance region.

B. Purity entanglement measure

As it is introduced in Ref. [21], the purity entanglement measure $u(N)$ purity is a good measure of generalized entanglement to capture the phase transition in the XY model in a transverse field. When the ground state of the system is unentangled, the purity is one, while zero purity means the ground state of the system is fully entangled. Moreover, the properties of the $u(N)$ purity has been investigated in Ref. [22] for the XY model in the presence of a time-dependent magnetic field, and show that this measure still captures the relevant correlations of the system and gives information about the physics underlying the evolution. Now, following the route provided in Ref. [22], the $u(N)$ purity of the time evolved state in Eq. (9) is given as

$$P_{u(N)} = \frac{2}{\pi} \int_0^\pi \left(v_k(t,\omega) v_k^*(t,\omega) - \frac{1}{2} \right)^2 dk. \tag{21}$$

Our calculation shows that the purity measure of a state [Eq. (9)] is time independent which is plotted in Fig. 6(a) versus driven frequency for Hamiltonian parameters $\mathcal{W} = \pi$ and $\mu = \pi/2$. As reflected, the purity measure, in the resonance regime, has a nonzero constant value but is less than one which means the time evolved ground state of the system is entangled. In the nonresonance region, the purity measure goes to one as the absolute value of driven frequency increases. In such a case, the ground state of the time-dependent Hamiltonian Eq. (1) is unentangled. The corresponding derivative of purity measure with respect to the driven frequency is also plotted in Fig. 6(b) versus driven frequency. As is clear, the derivative of the purity measure shows a discontinuity at the boundary of the resonance region. Therefore, the derivative of the purity measure can truly capture the boundary of the resonance region where DQPTs occur.
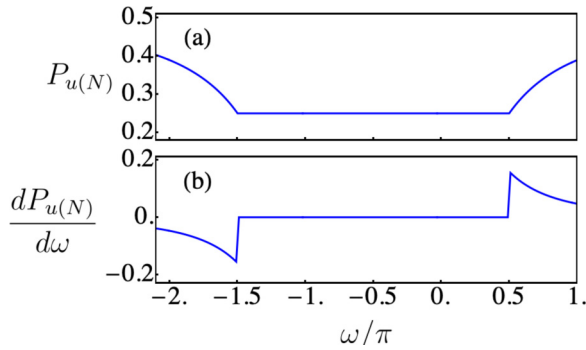
FIG. 6. (a) The purity entanglement measure and (b) its derivative with respect to driven frequency versus ω, for $\mathcal{W} = \pi$ and $\mu = \pi/2$.

V. CONCLUSION

We have investigated both pure and mixed states Floquet dynamical quantum phase transition in the one-dimensional p-wave superconductor with a time-driven pairing phase. The proposed time-dependent fermions system is equivalent to noninteracting quasispins imposed by a time-dependent effective magnetic field in Fourier space. We have shown that there exists a range of driven frequency over which the quasispins

are resonance. In the resonance region, the population of spin down and up states completely is a cycle and both states can be completely populated. While in the nonresonance regime spin-flip (Rabi transition) probability is less than the maximum possible value 1 and the state in which the system is initially prepared is never completely depopulated. We have also shown that there is a range of driving frequency where dynamical topological quantum phase transitions appear, without requiring any quantum quenches and that range corresponds to the resonance regime. Moreover, we study the entanglement spectrum and purity measure entanglement. The results state that the region where the Floquet dynamical topological quantum phase transitions arise is signaled by the degeneracy of the entanglement spectrum. In addition, derivative of the entanglement spectrum/purity entanglement measure with respect to the driven frequency shows divergence/discontinuity at the boundary of resonance regime.

[1] S. Sachdev, in *The Handbook of Magnetism and Advanced Magnetic Materials*, edited by H. Kronmuller and S. Parkin (Wiley, New York, 2007).

[2] M. Vojta, Rep. Prog. Phys. **66**, 2069 (2003).

[3] M. A. Nielsen and I. L. Chuang (Cambridge University Press, Cambridge, 2000), Vol. 2, p. 23.

[4] S. Campbell, J. Richens, N. L. Gullo, and T. Busch, Phys. Rev. A **88**, 062305 (2013).

[5] J. Preskill, J. Mod. Opt. **47**, 127 (2000).

[6] R. Jafari and A. Akbari, Phys. Rev. A **101**, 062105 (2020).

[7] S. Mahdavifar, S. Mahdavifar, and R. Jafari, Phys. Rev. A **96**, 052303 (2017).

[8] R. Jafari and A. Akbari, Europhys. Lett. **111**, 10007 (2015).

[9] U. Mishra, H. Cheraghi, S. Mahdavifar, R. Jafari, and A. Akbari, Phys. Rev. A **98**, 052338 (2018).

[10] E. Schrödinger, Math. Proc. Cambr. Philos. Soc. **31**, 555 (1935).

[11] A. Osterloh, L. Amico, G. Falci, and R. Fazio, Nature (London) **416**, 608 (2002).

[12] L.-A. Wu, M. S. Sarandy, and D. A. Lidar, Phys. Rev. Lett. **93**, 250404 (2004).

[13] R. Jafari, M. Kargarian, A. Langari, and M. Siahatgar, Phys. Rev. B **78**, 214414 (2008).

[14] G. Vidal, J. I. Latorre, E. Rico, and A. Kitaev, Phys. Rev. Lett. **90**, 227902 (2003).

[15] T. J. Osborne and M. A. Nielsen, Phys. Rev. A **66**, 032110 (2002).

[16] F. Verstraete, M. Popp, and J. I. Cirac, Phys. Rev. Lett. **92**, 027901 (2004).

[17] P. Zanardi and X. Wang, J. Phys. A: Math. Gen. **35**, 7947 (2002).

[18] S.-J. Gu, S.-S. Deng, Y.-Q. Li, and H.-Q. Lin, Phys. Rev. Lett. **93**, 086402 (2004).

[19] A. Anfossi, P. Giorda, and A. Montorsi, Phys. Rev. B **75**, 165106 (2007).

[20] H. Barnum, E. Knill, G. Ortiz, R. Somma, and L. Viola, Phys. Rev. Lett. **92**, 107902 (2004).

[21] R. Somma, G. Ortiz, H. Barnum, E. Knill, and L. Viola, Phys. Rev. A **70**, 042311 (2004).

[22] J. Batle, C. H. Raymond Ooi, and S. Abdalla, Phys. Rev. A **92**, 062341 (2015).

[23] Z. Gong and M. Ueda, Phys. Rev. Lett. **121**, 250601 (2018).

[24] H. Li and F. D. M. Haldane, Phys. Rev. Lett. **101**, 010504 (2008).

[25] P.-Y. Chang, J.-S. You, X. Wen, and S. Ryu, Phys. Rev. Res. **2**, 033069 (2020).

[26] V. M. Stojanović, Phys. Rev. B **101**, 134301 (2020).

[27] S. Lu and J. Yu, Phys. Rev. A **99**, 033621 (2019).

[28] M. Heyl, A. Polkovnikov, and S. Kehrein, Phys. Rev. Lett. **110**, 135704 (2013).

[29] M. Heyl, Rep. Prog. Phys. **81**, 054001 (2018).

[30] R. Jafari, H. Johannesson, A. Langari, and M. A. Martin-Delgado, Phys. Rev. B **99**, 054302 (2019).

[31] R. Jafari and H. Johannesson, Phys. Rev. Lett. **118**, 015701 (2017).

[32] U. Divakaran, Phys. Rev. E **88**, 052122 (2013).

[33] X.-Y. Hou, Q.-C. Gao, H. Guo, Y. He, T. Liu, and C.-C. Chien, Phys. Rev. B **102**, 104305 (2020).

[34] K. Najafi, M. A. Rajabpour, and J. Viti, Phys. Rev. B **97**, 205103 (2018).

[35] K. Najafi, M. A. Rajabpour, and J. Viti, J. Stat. Mech. (2019) 083102.

[36] B. Yan, L. Cincio, and W. H. Zurek, Phys. Rev. Lett. **124**, 160603 (2020).

[37] T. V. Zache, N. Mueller, J. T. Schneider, F. Jendrzejewski, J. Berges, and P. Hauke, Phys. Rev. Lett. **122**, 050403 (2019).

[38] S. Mukherjee and T. Nag, J. Stat. Mech. (2019) 043108.

[39] J. M. Zhang and H.-T. Yang, Europhys. Lett. **116**, 10008 (2016).

[40] J. M. Zhang and H.-T. Yang, Europhys. Lett. **114**, 60001 (2016).

[41] M. Serbyn and D. A. Abanin, Phys. Rev. B **96**, 014202 (2017).

[42] R. Jafari, J. Phys. A: Math. Theor. **49**, 185004 (2016).

[43] F. Andraschko and J. Sirker, Phys. Rev. B **89**, 125120 (2014).

[44] N. Sedlmayr, M. Fleischhauer, and J. Sirker, Phys. Rev. B **97**, 045147 (2018).

[45] S. Vajna and B. Dóra, Phys. Rev. B **91**, 155127 (2015).

[46] R. Jafari, Sci. Rep. **9**, 2871 (2019).

[47] J. C. Budich and M. Heyl, Phys. Rev. B **93**, 085416 (2016).

[48] X.-Y. Xu, Q.-Q. Wang, M. Heyl, J. C. Budich, W.-W. Pan, Z. Chen, M. Jan, K. Sun, J.-S. Xu, Y.-J. Han, C.-F. Li, and G.-C. Guo, Light: Sci. Appl. **9**, 7 (2020).

[49] S. Bhattacharjee and A. Dutta, Phys. Rev. B **97**, 134306 (2018).

[50] S. Sharma, A. Russomanno, G. E. Santoro, and A. Dutta, Europhys. Lett. **106**, 67003 (2014).

[51] U. Bhattacharya, S. Bandyopadhyay, and A. Dutta, Phys. Rev. B **96**, 180303(R) (2017).

[52] S. Sharma, U. Divakaran, A. Polkovnikov, and A. Dutta, Phys. Rev. B **93**, 144306 (2016).

[53] I. Homrighausen, N. O. Abeling, V. Zauner-Stauber, and J. C. Halimeh, Phys. Rev. B **96**, 104436 (2017).

[54] L. Zhou, Q.-H. Wang, H. Wang, and J. Gong, Phys. Rev. A **98**, 022129 (2018).

[55] B. Zhou, C. Yang, and S. Chen, Phys. Rev. B **100**, 184313 (2019).

[56] B. Mera, C. Vlachou, N. Paunković, V. R. Vieira, and O. Viyuela, Phys. Rev. B **97**, 094110 (2018).

[57] A. Khatun and S. M. Bhattacharjee, Phys. Rev. Lett. **123**, 160603 (2019).

[58] N. Sedlmayr, P. Jaeger, M. Maiti, and J. Sirker, Phys. Rev. B **97**, 064304 (2018).

[59] T. Masłowski and N. Sedlmayr, Phys. Rev. B **101**, 014301 (2020).

[60] M. Abdi, Phys. Rev. B **100**, 184310 (2019).

[61] K. Cao, W. Li, M. Zhong, and P. Tong, Phys. Rev. B **102**, 014207 (2020).

[62] S. Bhattacharyya and S. Dasgupta, J. Phys. A: Math. Theor. **53**, 265002 (2020).

[63] P. Uhrich, N. Defenu, R. Jafari, and J. C. Halimeh, Phys. Rev. B **101**, 245148 (2020).

[64] C. Rylands and V. Galitski [Special Issue Ann. Phys. (to be published)], arXiv:2001.10084.

[65] H. Hu and E. Zhao, Phys. Rev. Lett. **124**, 160402 (2020).

[66] L. Pastori, S. Barbarino, and J. C. Budich, Phys. Rev. Res. **2**, 033259 (2020).

[67] T. H. Kyaw, V. M. Bastidas, J. Tangpanitanon, G. Romero, and L.-C. Kwek, Phys. Rev. A **101**, 012111 (2020).

[68] U. Mishra, R. Jafari, and A. Akbari, J. Phys. A: Math. Theor. **53**, 375301 (2020).

[69] R. Puebla, Phys. Rev. B **102**, 220302(R) (2020).

[70] C. Ding, Phys. Rev. B **102**, 060409(R) (2020).

[71] N. Fläschner, D. Vogel, M. Tarnowski, B. S. Rem, D.-S. Lühmann, M. Heyl, J. C. Budich, L. Mathey, K. Sengstock, and C. Weitenberg, Nat. Phys. **14**, 265 (2017).

[72] P. Jurcevic, H. Shen, P. Hauke, C. Maier, T. Brydges, C. Hempel, B. P. Lanyon, M. Heyl, R. Blatt, and C. F. Roos, Phys. Rev. Lett. **119**, 080501 (2017).

[73] E. A. Martinez, C. A. Muschik, P. Schindler, D. Nigg, A. Erhard, M. Heyl, P. Hauke, M. Dalmonte, T. Monz, P. Zoller *et al.*, Nature (London) **534**, 516 (2016).

[74] X.-Y. Guo, C. Yang, Y. Zeng, Y. Peng, H.-K. Li, H. Deng, Y.-R. Jin, S. Chen, D. Zheng, and H. Fan, Phys. Rev. Appl. **11**, 044080 (2019).

[75] K. Wang, X. Qiu, L. Xiao, X. Zhan, Z. Bian, W. Yi, and P. Xue, Phys. Rev. Lett. **122**, 020501 (2019).

[76] X. Nie, B.-B. Wei, X. Chen, Z. Zhang, X. Zhao, C. Qiu, Y. Tian, Y. Ji, T. Xin, D. Lu, and J. Li, Phys. Rev. Lett. **124**, 250601 (2020).

[77] T. Tian, H.-X. Yang, L.-Y. Qiu, H.-Y. Liang, Y.-B. Yang, Y. Xu, and L.-M. Duan, Phys. Rev. Lett. **124**, 043001 (2020).

[78] F. X. Sun, W. Zhang, Q. Y. He, and Q. H. Gong, Phys. Rev. A **97**, 012307 (2018).

[79] S. De Nicola, A. A Michailidis, and M. Serbyn, arXiv:2008.04894.

[80] M. Schmitt and S. Kehrein, Phys. Rev. B **92**, 075114 (2015).

[81] E. Canovi, E. Ercolessi, P. Naldesi, L. Taddia, and D. Vodola, Phys. Rev. B **89**, 104303 (2014).

[82] G. Torlai, L. Tagliacozzo, and G. D. Chiara, J. Stat. Mech. (2014) P06001.

[83] J. Surace, L. Tagliacozzo, and E. Tonni, Phys. Rev. B **101**, 241107(R) (2020).

[84] K. Su, Z.-H. Sun, and H. Fan, Phys. Rev. A **101**, 063613 (2020).

[85] A. Kosior and K. Sacha, Phys. Rev. A **97**, 053621 (2018).

[86] A. Kosior, A. Syrwid, and K. Sacha, Phys. Rev. A **98**, 023612 (2018).

[87] K. Yang, L. Zhou, W. Ma, X. Kong, P. Wang, X. Qin, X. Rong, Y. Wang, F. Shi, J. Gong, and J. Du, Phys. Rev. B **100**, 085308 (2019).

[88] S. Zamani, R. Jafari, and A. Langari, Phys. Rev. B **102**, 144306 (2020).

[89] A. Y. Kitaev, Phys. Usp. **44**, 131 (2001).

[90] Y. O. Nakagawa, G. Misguich, and M. Oshikawa, Phys. Rev. B **93**, 174310 (2016).

[91] J. Schwinger, Phys. Rev. **51**, 648 (1937).

[92] M. Rodriguez-Vega, M. Lentz, and B. Seradjeh, New J. Phys. **20**, 093022 (2018).

[93] M. E. Fisher, Rep. Prog. Phys. **30**, 615 (1967).

[94] M. Heyl and J. C. Budich, Phys. Rev. B **96**, 180304(R) (2017).

[95] H. Lang, Y. Chen, Q. Hong, and H. Fan, Phys. Rev. B **98**, 134310 (2018).

[96] L. Amico, R. Fazio, A. Osterloh, and V. Vedral, Rev. Mod. Phys. **80**, 517 (2008).

[97] T. L. Hughes, E. Prodan, and B. A. Bernevig, Phys. Rev. B **83**, 245132 (2011).

[98] L. Fidkowski, Phys. Rev. Lett. **104**, 130502 (2010).